Check for updates

Which Parameters Determine the Low-Light Behaviour of CIGSSe-Based Thin-Film Solar Cells?

Stephan J. Heise*, Teoman Taskesen , Abdel Kader Ndoukoue Chintouo and Jörg Ohland

Ultrafast Nanoscale Dynamics, Institute of Physics, University of Oldenburg, Oldenburg, Germany

The performance of solar cells in realistic operating conditions usually differs from the specified efficiency at standard test conditions (STC). Among other factors, the illumination intensity (irradiance) is often lower than at STC, which leads to a lower device efficiency. Therefore, it becomes important to optimize the output power at low-light conditions in order to achieve a high energy yield at a specific location. For this purpose, it is essential to have a detailed knowledge of the relevant parameters that govern the low-light behaviour. This study investigates the impact of the diode parameters on the low-light performance of thin-film solar cells based on chalcopyrite $Cu(In,Ga)(S,Se)_2$ absorbers. Experimental irradiance-dependent current-voltage results are analysed with the help of an analytical model. For each parameter the contributions of its absolute value and its irradiance dependence are assessed. Additionally, relations between the diode parameters and material parameters are examined by analysing different cell variations. The results show that cell performance at low-light conditions is primarily governed by the irradiance dependence of the fill factor, which in turn is mainly determined by the parallel resistance of the device. Moreover, a reduction of the dark saturation current and the ideality factor towards lower irradiances is observed which indicates an irradiance-dependent change of recombination dynamics. The consequence is an increase of the open-circuit voltage at low-light conditions which indirectly also boosts the fill factor. The results suggest that cell optimization for low-light conditions should focus on improving the parallel resistance and tuning recombination in a way that the dark saturation current decreases with decreasing irradiance.

Keywords: thin-film solar cell (TFSC), CIGSSe, low-light behaviour, Shockley model, current, voltage (I-V) characteristic

INTRODUCTION

The performance of photovoltaic (PV) modules is commonly rated at standard test conditions (STC), i.e. at 25°C and a 1000 W/m²-illumination with an AM1.5 spectrum (IEC 60904-3, 2019). However, in realistic field situations these conditions are hardly ever met: Regarding the irradiance, for instance, 1000 W/m² are rarely reached in parts of the world with a latitude beyond 55° (Honsberg and Bowden, 2022), such as Northern Europe, Russia or Canada. And for indoor applications typical irradiances are even below 5 mW/m² (Virtuani et al., 2003). Moreover, performance losses due to higher ambient temperatures (Ahmed et al., 2021)

increase towards lower irradiances (Farias-Basulto et al., 2020; Ahmed et al., 2022). So in order to actually achieve a high energy yield of a PV module, in many situations it is critical to ensure a high performance at irradiances lower than 1000 W/m^2, which will be referred to as a device's *low-light behaviour* in this article.

For improving the low-light behaviour of a specific cell technology, a detailed knowledge about the governing mechanisms and parameters is needed. To this end, the irradiance dependence of the efficiency may be broken down into the irradiance dependences of the short-circuit current density J_{SC}, of the open-circuit voltage V_{OC}, and of the fill factor FF. While the J_{SC} scales directly linearly with the irradiance ϕ, the irradiance dependences of V_{OC} and FF are influenced by material and device parameters, such as non-radiative recombination and the parallel resistance R_p.

Many studies have been conducted to assess and to model the irradiance dependence of the main IV parameters. This has mostly been done for silicon solar cells (Grunow et al., 2004; Chegaar et al., 2013; Litzenburger et al., 2014; Fébba et al., 2018; Anani and Ibrahim, 2020), but also a few reports for chalcopyrite (Virtuani et al., 2003; Liu et al., 2009; Farias-Basulto et al., 2020) and CdTe (Shen et al., 2014) solar cells exist. A general finding is that particularly the parallel resistance R_p is most critical for the low-light behaviour in all technologies (Feurer et al., 2017). However, so far it is not fully clear, whether the absolute value of this parameter is more crucial, or whether its irradiance dependence also plays an important role.

In this study we analyse a variety of thin-film solar cells based on Cu(In,Ga)(S,Se)$_2$ (CIGSSe) absorber layers in order to determine the most important diode parameters that govern the low-light behaviour of these cells. The investigated parameters include the primary and secondary current-voltage (IV) parameters, i.e. J_{SC}, V_{OC}, and FF as well as series resistance R_s, parallel resistance R_p, dark saturation current density J_0 and ideality factor A. First, we analyse experimental results of the different cell variations in order to associate device parameters with the underlying material physics. In a second part, we make use of an analytical model to separately assess the influence of a specific parameter's value at STC on the one hand and of its irradiance dependence on the other.

METHODS

Experimental

The samples used in this study were fabricated with the typical layer structure of: glass substrate | Mo back contact | absorber | buffer | intrinsic ZnO | ZnO:Al. The CIGSSe absorber layers were grown using a rapid-thermal processing (RTP) of stacked elemental metal layers (for more details on the process the interested reader is referred to Dalibor et al., 2016). Four different cell types (labelled A, C, D, E) were generated by modifying individual cell layers, e.g. by varying the Ga and S content in the absorber layer or by omitting the i-ZnO layer. An overview of the cell types is given in **Table 1**. The samples had an active area of

TABLE 1 | Overview of the cell types used in this study.

Cell Type	A	C	D	E
ZnO:Al	✗	✗	✗	✗
i-ZnO	✗	✗	—	—
Buffer	InS:Na	Zn(O,S)	Zn(O,S)	Zn(O,S)
CIGSSe	low Ga, S	high Ga, S	high Ga, S	high Ga, S
Back contact	Cu-based	Cu-based	Cu-based	Mo-based
# samples	3	3	1	3

≈0.9 cm^2 and were cut from 30×30-cm^2 minimodules. One to three samples per cell type were investigated.

Current-voltage measurements were performed by illuminating the samples with a AAA solar simulator (PET SS100AAA) whose intensity was calibrated by a Si reference cell to match 1000 W/m^2. To achieve different low-light conditions, the irradiance on the samples was varied by placing neutral density filters in the optical path. The resulting irradiances at the sample position were determined by the Si reference cell. Throughout the measurements the samples' temperature was kept at 25.0 ± 0.2°C by monitoring a thermocouple on a nearby dummy cell and adjusting the water-heated sample stage. The cells were contacted by metal contact bands on neighbouring cells via the monolithic series interconnects. A source-measure unit (Keithley 2400) was used to apply voltages and measure currents in a four-probe contacting scheme. Prior to the IV measurements, the samples were pre-conditioned ("light-soaked") under 1000 W/m^2 illumination at 25°C for 2 hours in order to exclude metastable changes during the measurements as much as possible. Cell areas were determined from digital images.

Secondary IV parameters were determined by a least-squares fit of the Shockley diode equation (including resistances) to the measured IV data, for which the results of the Hegedus method (Hegedus and Shafarman, 2004) served as start parameters.

Model

The secondary IV parameters obtained from experiment were used as input parameters to model the V_{OC} and the FF via (Green, 1992)

$$V_{OC} = \frac{AkT}{q}\ln\left(\frac{J_{SC}}{J_0}\right) \tag{1}$$

and

$$FF = FF_0\left(1 - r_s\right)\left(1 - \frac{(v_{oc} + 0.7)}{v_{oc}}\frac{FF_0\left(1 - r_s\right)}{r_p}\right) \tag{2}$$

where $v_{oc} := qV_{OC}/AkT$, $r_{s,p} := R_{s,p} \cdot J_{SC}/V_{OC}$, and $FF_0 := [v_{oc} - \ln(v_{oc} + 0.72)]/(v_{oc} + 1)$. Here, q is the elementary charge, k the Boltzmann constant, and T the sample temperature. In order to model the irradiance dependence, the experimental J_{SC} was used in **Eqs. 1, 2**. Then, the model was either fed with constant parameter values (STC) for all irradiances, or with the irradiance-dependent parameter values.

RESULTS

First, we analyse the experimentally obtained low-light behaviour of the 4 cell types, which is shown in **Figure 1A**. Here, the irradiances ϕ and the efficiencies η are normalized to their respective values at STC. It is apparent, that for irradiances below 40% the low-light behaviour may differ quite significantly between the different cell types. Whereas cell types A and especially C have a rather constant efficiency down to $\phi = 13\%$, cell types D and E show an earlier and also larger drop in efficiency. A very similar trend is observed for the irradiance dependence of the *FF* (**Figure 1B**). The $V_{OC}(\phi)$ data, however, show much less variation between the cell types. Taken together, this suggests that the efficiency at low irradiances is essentially governed by the values of the *FF*.
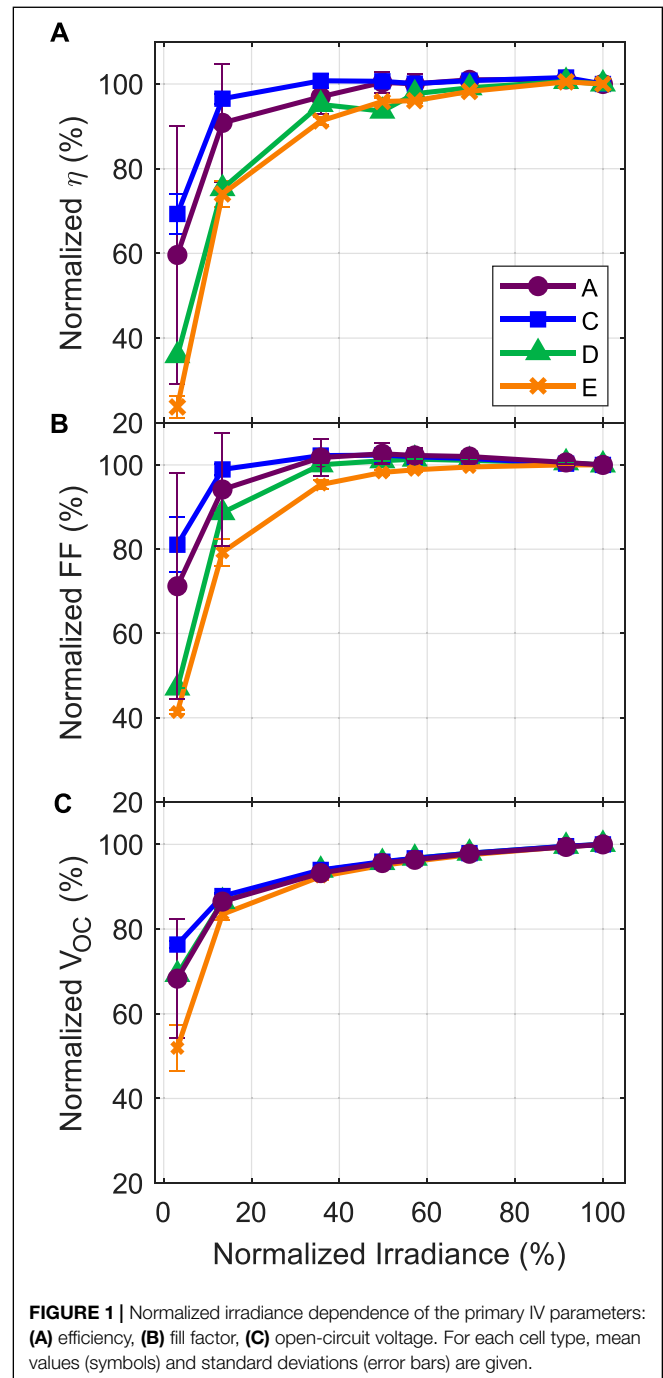
In order to understand what mechanisms contribute to the irradiance dependence of the fill factor, we next analyse the secondary IV parameters (**Figure 2**), since the *FF* is influenced by R_s and R_p directly, and by J_0 and A indirectly via the V_{OC} (c.f. **Eqs. 1**, **2**).
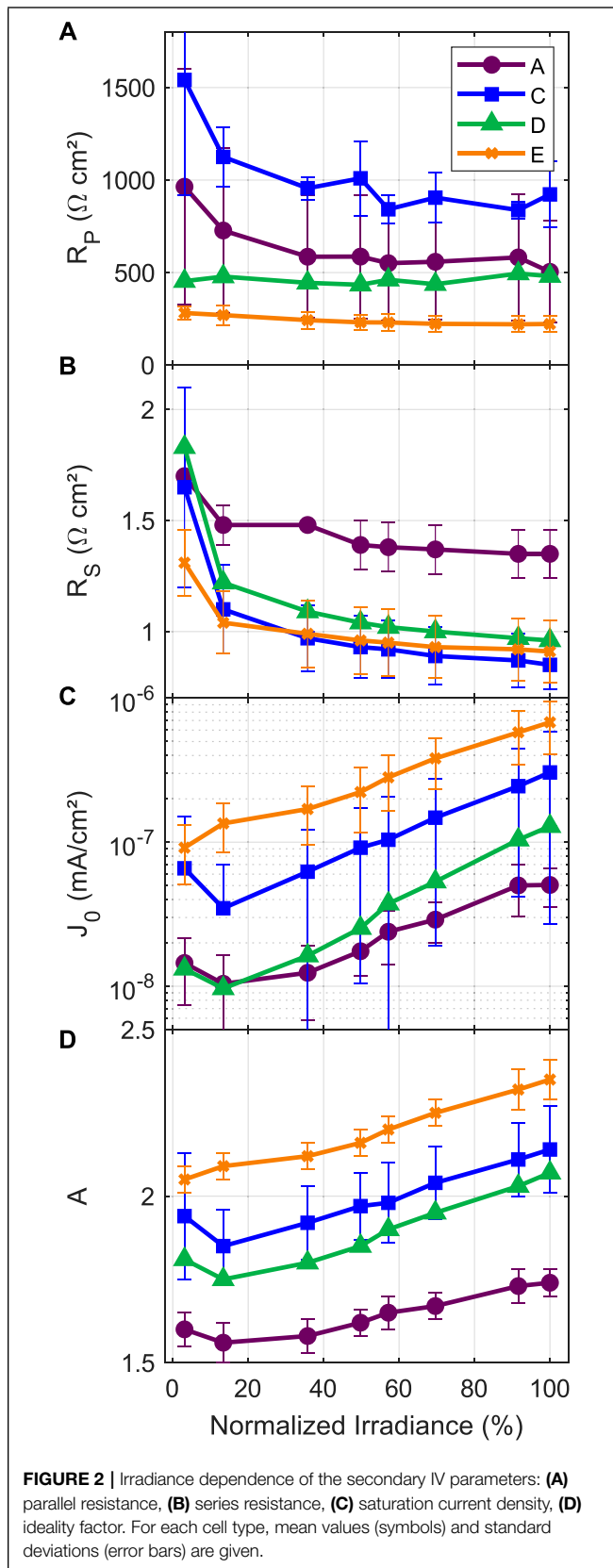
An analysis of the parallel resistance R_p (**Figure 2A**) directly shows, that the absolute values of R_p correlate with the relative values of the *FF* at low irradiances, reflecting the commonly acknowledged relation that a high R_p leads to a good low-light behaviour (see e.g. Grunow et al., 2004): Cell types A and C have a higher R_p and also less *FF* loss at low ϕ than cell types D and E. This could be an effect of the intrinsic ZnO layer which is omitted in cell types D and E (c.f. **Table 1**), thus facilitating shunt currents via, e.g., increased interface recombination. Modifications of other cell layers do not seem to show a systematic influence on the R_p.

However, in addition to the differences in *absolute* R_p, we also see a difference in the *shape* of the $R_p(\phi)$ curves between these two groups of cell types. For cell types A and C the R_p increases noticeably towards lower irradiances. It should be noted here that, despite the large error bars in **Figure 2**, the trends for the individual samples of a cell type are very similar and mostly their absolute values vary. Judging from data reported in the literature, this increasing R_p seems to be the "normal" behaviour in chalcopyrite (Virtuani et al., 2003; He et al., 2007; Liu et al., 2009; Schubbert et al., 2016) and also silicon (Chegaar et al., 2013) solar cells. In contrast, cell types D and E show a nearly constant irradiance dependence.

For interpreting these results it is important to keep in mind that the parallel resistance R_p is a lumped circuit-model representation of various losses that occur in parallel with the main diode (Shen et al., 2014). Virtuani et al. (2003) relate the irradiance dependence of the R_p to the irradiance-dependent photoconductivity of the absorber material. Schubbert et al. (2016) confirmed this idea in simulations of shunt currents across the P1 trench (which separates the back electrode in CIGSSe modules in order to create a monolithic series interconnection of the individual cells). They showed that the irradiance dependence of the R_p is influenced by the doping density of the absorber material and the width of the P1 trench. This suggests that the different $R_p(\phi)$ shapes might be due to differences in doping density. However, capacitance-voltage

measurements (not shown) revealed that the doping densities of cell types A, C, and D are virtually identical, and only cell type E shows a slightly higher (1.3×) doping density (Stölzel, 2021). Therefore it seems likely that the irradiance dependence of the R_p is controlled by other mechanisms in our cells. Shen et al. (2014) observed a very similar behaviour in CdTe solar cells: In a device with a high parallel resistance the $R_p(\phi)$ showed a power-law increase towards lower irradiances, whereas in a device with a low R_p it stayed nearly constant. From equivalent-circuit modelling

FIGURE 1 | Normalized irradiance dependence of the primary IV parameters: **(A)** efficiency, **(B)** fill factor, **(C)** open-circuit voltage. For each cell type, mean values (symbols) and standard deviations (error bars) are given.

FIGURE 2 | Irradiance dependence of the secondary IV parameters: **(A)** parallel resistance, **(B)** series resistance, **(C)** saturation current density, **(D)** ideality factor. For each cell type, mean values (symbols) and standard deviations (error bars) are given.

they concluded that the main difference was the existence of a weak diode in the device with a low R_p. Possibly, the situation is similar in our devices and the weak diode is related to the omitted i-ZnO layer.

However, independent of the origin of the R_p behaviour, the question arises, whether the better low-light behaviour of cell types A and C is due to their higher absolute R_p or due to their increase in R_p towards lower irradiances. This will be addressed below in the modelling section.

The series resistance R_s (**Figure 2B**) increases towards lower irradiances for all investigated cell types. This behaviour is in line with findings reported in literature (Virtuani et al., 2003; Liu et al., 2009), and probably reflects a reduction of the photoconductivity of the Al-doped ZnO front contact layer upon decreasing the irradiance. Correspondingly, this trend is not observed in silicon devices (Chegaar et al., 2013; Fébba et al., 2018). Regarding the absolute values, cell type A shows a somewhat higher R_s than the other cell types for most irradiances. However, it seems that this does not have any noticeable effect on the *FF*: At STC, *FF(A)* = 65.9% is only slightly lower than *FF(D)* = 67.3% and even higher than *FF(E)* = 63.2%. Apparently, R_s is low enough to not be a limiting factor here.

The dark saturation current J_0 and the ideality factor *A* contain information about recombination processes in the device and are thus expected to affect mostly the V_{OC}. In the investigated cell types, J_0 and *A* consistently decrease with decreasing irradiance (**Figure 2C+d**), which implies that the amount of recombination (J_0) as well as the place of the dominant recombination (*A*) change as a function of irradiance. This suggests a generation-dependent activity of certain recombination channels, which does not seem to be present in previous findings (Virtuani et al., 2003; Liu et al., 2009). This issue is investigated in more detail in a separate study (Ahmed et al., 2022), which indicates that the location of the dominant recombination plays a crucial role for the low-light behaviour and may slightly shift with varying irradiance. The variation in the absolute values of J_0 and *A* between the cell types does not show any direct correlation to the V_{OC} values at STC (not shown). This is probably because the V_{OC} is not only influenced by recombination alone, but also by the absorber's band gap and doping density which may counterbalance changes in recombination.

To summarize, the analysis has shown that nearly all secondary parameters seem to change upon changing the irradiance. In addition, their absolute values at STC often differ between cell types. In order to further understand the individual contributions of a) the absolute value and b) the irradiance dependence of these parameters to the low-light behaviour, we make use of an analytic model in the following.

The idea is to model the irradiance dependence of the V_{OC} and the *FF* according to **Eqs. 1**, **2**, and feed the model either with constant parameter values (STC) for all irradiances, or with the irradiance-dependent parameter values. Particularly for the R_p, where we observed two different trends of irradiance dependences, it is interesting to be able to differentiate between effects of absolute value and irradiance dependence. Therefore
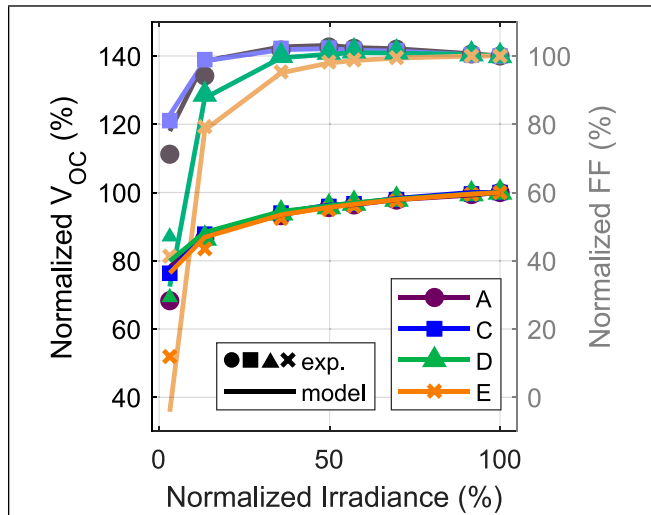
FIGURE 3 | Model quality: Comparison of the full model (lines) with the mean experimental data (symbols) of the 4 cell types (color-coded) for the V_{OC} (left axis) and the *FF* (right axes).
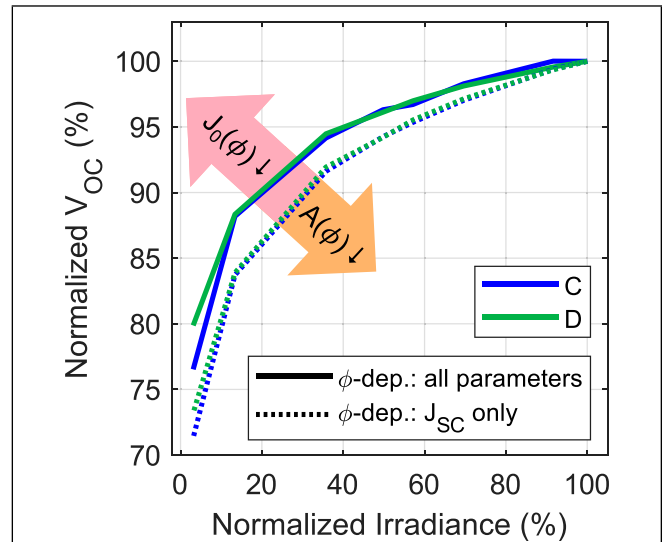

FIGURE 4 | Modelling the V_{OC} of cell types C (blue) and D (green) including the irradiance dependence of either all parameters (solid lines) or of J_{SC} only (dotted lines).

we chose one data set for each trend, cell types C and D, for the modelling.

In a first step, we checked whether the model is able to adequately describe the devices used in this study. Since **Eq 1** is derived from the Shockley equation for *ideal* diodes and **Eq 2** is an *empirical* finding from *silicon* cells, this is an important precaution (although the criteria for an accuracy of at least two significant digits in **Eq. 2**—$v_{oc} > 10$, $r_s < 0.4$, $r_p > 2.5$ (Green, 1992)—are met here). Therefore we tested, whether the experimental results are reproduced by the model, if the irradiance-dependent data of all input parameters (J_{SC}, R_p, R_s, J_0, A) was used. A comparison of experimental and modelled results for this case is shown in **Figure 3**. The data show that apart from some deviations at the lowest irradiance ($\phi_{min} = 3\%$), the model is in good agreement with the measurements, so that it seems to reflect the basic behaviour of the cells decently.

For modelling the open-circuit voltage we start by using fixed STC values for all input parameters except J_{SC} (for J_{SC}, the irradiance-dependent data are used in all cases to reproduce the basic irradiance dependence). The results are shown in **Figure 4** (dotted lines). We note, that the irradiance dependence of V_{OC} is effectively the same for both cell types, i.e. it seems to be independent of the absolute values of J_0 and A which differ between the cell types C and D (cf. **Figure 2**). If we include the irradiance dependence of the resistances R_p and R_s next, the results do not change (not shown), which indicates that the resistances do not play a role for the V_{OC}'s low-light behaviour. However, if the irradiance dependences of the diode parameters J_0 and A are included, the V_{OC} results change noticeably (solid lines in **Figure 4**): Upon reducing the irradiance, the ideality factor A decreases, which leads to a reduction of the V_{OC} (indicated by the orange arrow in **Figure 4**). At the same time, J_0 also decreases, which results in an increase of V_{OC} that effectively outweighs
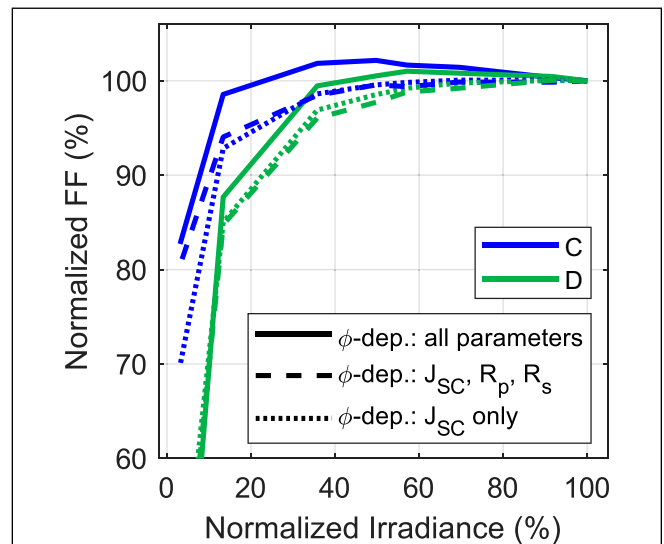

FIGURE 5 | Modelling the *FF* of cell types C (blue) and D (green) including the intensity dependence of either all parameters (solid lines), of J_{SC}, R_s and R_p (dashed lines), or of J_{SC} only (dotted lines).

the reduction due to the decreasing A. In consequence, the V_{OC}-decrease towards low irradiances is less than if $J_0(\phi)$ and $A(\phi)$ were constant. This shows that the irradiance dependence of J_0 and A can have a significant effect on the low-light characteristics of the V_{OC}. Since the 2 cell types exhibit a very similar irradiance dependence of J_0 and A, the V_{OC} results here are very similar, too.

The modelling results for the fill factor are given in **Figure 5**. Here, the scenario where all input parameters are fixed at their STC values (dotted lines) shows a significant difference in the $FF(\phi)$ characteristics between the 2 cell types. Since the R_s values are very similar for these cell types but the R_p values differ by

nearly a factor of 2, this result demonstrates the importance of the absolute value of the parallel resistance for the irradiance dependence of the *FF*. The minor role of the R_s is in line with findings for silicon solar cells which report that the series resistance only limits the low-light performance if limitations due to the parallel resistance are negligible (Litzenburger et al., 2014).

If we include the irradiance dependence of the resistances (dashed lines in **Figure 5**), we see hardly any difference for most irradiances. However, at very low irradiances the increase of R_p in cell type C seems to lead to an increase in *FF*, which is not observed for cell type D where $R_p(\phi) \approx const$. In the last case, where additionally the irradiance dependences of J_0 and A are included in the model (solid lines in **Figure 5**), a significant increase of the *FF* is seen for irradiances below $\phi = 100\%$. This may be explained by the impact of $J_0(\phi)$ and $A(\phi)$ on the low-light characteristics of the V_{OC} (see above) which indirectly also seems to largely affect the low-light characteristics of the *FF*.

CONCLUSION

In this study we investigated the impact of the primary and secondary IV parameters on the low-light behaviour of a variation of CIGSSe solar cells. By analysing the parameters extracted from measured IV characteristics and modelling them back with an analytical approach, we separately assessed the influence of the absolute value of a parameter at STC as well as its irradiance dependence.

Based on the obtained results, we suggest that an improvement of a device's low-light behaviour should focus mainly on two aspects:

1. Increase of the parallel (shunt) resistance R_p of the device at STC. This should lead to a higher fill factor at low-light conditions. Possible shunt paths to optimize in CIGSSe modules include the P1 scribe (Schubbert et al., 2016), grain boundaries (Williams et al., 2015) or defective areas due to material inhomogeneities (Richter et al., 2015). The results from the current study indicate that the intrinsic ZnO layer may promote a high R_p.
2. Decrease of the dark saturation current density J_0 with decreasing irradiance. This should lead to a higher open-circuit voltage at low-light conditions, and thus also increase the fill factor. Tuning J_0 is less straightforward because it implies modifications of the recombination dynamics. In the investigated cells

this effect might have been achieved by a slight irradiance-dependent shift in the dominating recombination's location (Ahmed et al., 2022).

Further, an increase in R_p towards lower irradiances may help to increase the *FF* at very low irradiances and could thus be attractive particularly for indoor applications. A decrease in ideality factor on the other hand leads to a decrease in V_{OC} which negatively affects the low-light behaviour. Finally, the series resistance R_s does not seem to have a significant impact on the low-light behaviour as long as its value is reasonably low.

This study showed which diode parameters mostly determine the low-light performance of the investigated CIGSSe solar cells. The results are often similar to what has been reported for silicon devices. For implementing the suggested parameter optimizations, it is necessary to understand how the diode parameters relate to material parameters and how to control the relevant material parameters during the fabrication process. By investigating the impact of different cell modifications, certain insights on this issue could be gained here; but it is apparent that additional research will be needed to further improve the low-light performance—and thus the energy yield—of CIGSSe thin-film solar cells.

DATA AVAILABILITY STATEMENT

The raw data supporting the conclusion of this article will be made available by the authors, without undue reservation.

AUTHOR CONTRIBUTIONS

SH supervised the study and wrote the manuscript. TT devised, implemented and analysed the modelling part of the study. AN did the IV measurements and their analysis. JO devised and supervised the IV measurement part of the study, and analysed the experimental data.

ACKNOWLEDGMENTS

REFERENCES

Ahmed, H., Elshabasi, M., Gonzalez, M. A., Richter, M., Stölzel, M., Weber, A., et al. (2022). Identifying Dominant Recombination Locations In Double-Graded Cu(In$_{1-x}$Ga$_x$)(Se$_{1-y}$S$_y$)$_2$ Solar Cells and Their Impact on the Performance at Different Light Intensities. *Prog. Photovoltaics* 30, 670–678. doi:10.1002/pip.3543

Ahmed, H., Elshabasi, M., Ohland, J., Stölzel, M., Weber, A., Lechner, R., et al. (2021). Temperature Coefficient Characterization of CIGSSe Solar

Cells with Layer Modifications. *Sol. Energy Mater. Sol. Cells* 225, 111059. doi:10.1016/j.solmat.2021.111059

Anani, N., and Ibrahim, H. (2020). Adjusting the Single-Diode Model Parameters of a Photovoltaic Module with Irradiance and Temperature. *Energies* 13, 3226. doi:10.3390/en13123226

Chegaar, M., Hamzaoui, A., Namoda, A., Petit, P., Aillerie, M., and Herguth, A. (2013). Effect of Illumination Intensity on Solar Cells Parameters. *Energy Procedia* 36, 722–729. doi:10.1016/j.egypro.2013.07.084

Dalibor, T., Eraerds, P., Grave, M., Algasinger, M., Visbeck, S., Niesen, T., et al. (2016). "Advanced PVD Buffers on the Road to GW-Scale CIGSSe Production," in IEEE 43rd Photovoltaic Specialists Conference (PVSC). doi:10.1109/pvsc.2016.7749853

Farias-Basulto, G. A., Reyes-Figueroa, P., Ulbrich, C., Szyszka, B., Schlatmann, R., and Klenk, R. (2020). Validation of a Multiple Linear Regression Model for CIGSSe Photovoltaic Module Performance and Pmpp Prediction. *Sol. Energy* 208, 859–865. doi:10.1016/j.solener.2020.08.040

Fébba, D. M., Rubinger, R. M., Oliveira, A. F., and Bortoni, E. C. (2018). Impacts of Temperature and Irradiance on Polycrystalline Silicon Solar Cells Parameters. *Sol. Energy* 174, 628–639. doi:10.1016/j.solener.2018.09.051

Feurer, T., Reinhard, P., Avancini, E., Bissig, B., Löckinger, J., Fuchs, P., et al. (2017). Progress in Thin Film CIGS Photovoltaics - Research and Development, Manufacturing, and Applications. *Prog. Photovolt. Res. Appl.* 25, 645–667. doi:10.1002/pip.2811

Green, M. A. (1992). *Solar Cells: Operating Principles, Technology and System Applications*. University of New South Wales, Sydney.

Grunow, P., Lust, S., Sauter, D., Hoffmann, V., Beneking, C., Litzenburger, B., et al. (2004). "Weak Light Performance and Annual Yields of PV Modules and Systems as a Result of the Basic Parameter Set of Industrial Solar Cells," in Proceedings of the 19th European Photovoltaic Solar Energy Conference (Paris), 2190–2193.

He, W., Sun, Y., Qiao, Z., Ao, J., Wang, X., and Li, C. (2007). J-V Characteristics of $Cu(In_{1-x}Ga_x)Se_2$ Thin Film Solar Cells. *Chin. J. Semicond.* 28, 1941.

Hegedus, S. S., and Shafarman, W. N. (2004). Thin-Film Solar Cells: Device Measurements and Analysis. *Prog. Photovolt. Res. Appl.* 12, 155–176. doi:10.1002/pip.518

Honsberg, C. B., and Bowden, S. G. (2022). Calculation of Solar Insolation. Available at: www.pveducation.org.

IEC 60904-3 (2019). *Photovoltaic Devices - Part 3: Measurement Principles for Terrestrial Photovoltaic (PV) Solar Devices with Reference Spectral Irradiance Data*. IEC 60904-3. *Int. Electrotech. Comm.*

Litzenburger, B., Pingel, S., Janke, S., Held, S., and Alam, R. (2014). "Low Light Performance of Solar Cells and Modules," in Proceedings of the 29th European Photovoltaic Solar Energy Conference and Exhibition, 3231–3236. doi:10.4229/EUPVSEC20142014-5CV.2.6

Liu, F.-F., Sun, Y., Zhang, L., Li, C.-J., Qiao, Z.-x., He, Q., et al. (2009). Study on Performance of Polycrystalline Cu(In,Ga)Se₂ Solar Cells under Different Irradiance. *J. Synthetic Cryst.* 38, 576–580. doi:10.16553/j.cnki.issn1000-985x.2009.03.052

Richter, M., Babbe, F.-S., Vetter, A., Heise, S. J., Ohland, J., and Riedel, I. (2015). "Origins of Shunt Signals of Cu(In,Ga)Se₂ Solar Cells Investigated by Two-Dimensional Simulations," in Proceedings of the 31st EUPVSEC. doi:10.4229/EUPVSEC20152015-3CO.6.3

Schubert, C., Eraerds, P., Richter, M., Parisi, J., Riedel, I., Dalibor, T., et al. (2016). Performance Ratio Study Based on a Device Simulation of a 2D Monolithic Interconnected Cu(In,Ga)(Se,S)₂ Solar Cell. *Sol. Energy Mater. Sol. Cells* 157, 146–153. doi:10.1016/j.solmat.2016.05.002

Shen, C., Kampwerth, H., and Green, M. A. (2014). Photoluminescence Based Open Circuit Voltage and Effective Lifetime Images Re-Interpretation for Solar Cells: The Influence of Horizontal Balancing Currents. *Sol. Energy Mater. Sol. Cells* 130, 393–396. doi:10.1016/j.solmat.2014.07.035

Stölzel, M., Heise, S.J., Hock, R., Wellmann, P., and Klenk, R. (2021). *Energieertragsoptimierte Cu(In,Ga)(S,Se)₂-Dünnschichtsolarmodule durch gezielte Steuerung der Ertragsparameter (MYCIGS)*. AVANCIS GmbH, München. doi:10.2314/KXP:1808058976

Virtuani, A., Lotter, E., and Powalla, M. (2003). Performance of Cu(In,Ga)Se₂ Solar Cells under Low Irradiance. *Thin Solid Films* 431-432, 443–447. doi:10.1016/S0040-6090(03)00184-6

Williams, B. L., Smit, S., Kniknie, B. J., Bakker, K. J., Keuning, W., Kessels, W. M. M., et al. (2015). Identifying Parasitic Current Pathways in CIGS Solar Cells by Modelling Dark J-V Response. *Prog. Photovolt. Res. Appl.* 23, 1516–1525. doi:10.1002/pip.2582